EVALUATION OF NUSSELT NUMBER FOR A FLOW IN A MICROTUBE USING SECOND-ORDER SLIP MODEL

by

Barbaros CETIN [a*] ***and Ozgur BAYER*** [b]

[a] Mechanical Engineering, Middle East Technical University – Northern Cyprus Campus, Guzelyurt, Turkey
[b] Department Mechanical Engineering, University of Kentucky, Lexington, Ken., USA

Original scientific paper
UDC: 532.517.2:536.23/.24:519.876.2
DOI: 10.2298/TSCI11S1103C

In this paper, the fully-developed temperature profile and corresponding Nusselt value is determined analytically for a gaseous flow in a microtube with a thermal boundary condition of constant wall heat flux. The flow assumed to be laminar, and hydrodynamically and thermally fully developed. The fluid is assumed to be constant property and incompressible. The effect of rarefaction, viscous dissipation and axial conduction, which are important at the microscale, are included in the analysis. Second-order slip model is used for the slip-flow and temperature jump boundary conditions for the implementation of the rarefaction effect. Closed form solutions for the temperature field and the fully-developed Nusselt number is derived as a function of Knudsen number, Brinkman number and Peclet number.

Key words: *microtube, rarefaction, second-order slip model, viscous dissipation, axial conduction*

Introduction

The recent developments in micro- and nano-fabrication techniques have enabled the usage of fluidic and thermal systems with micrometer dimensions in many biomedical and engineering applications such as micro-reactors, micro-heat exchangers, cell reactors *etc*. Therefore, the fundamental understanding of the transport phenomena at microscale is crucial to design, optimize and utilize improved micron-sized systems. Analysis of heat transfer inside a microtube is one of the fundamental problems to understand the fluid physics at microscale. There are several issues that need to be considered at microscale.

The ratio of the mean free path to the characteristic length, a dimensionless quantity, is known as Knudsen number (Kn = λ/L). As Knudsen number increases, fluid modeling is moving from continuum models to molecular models, and non-continuum effects needs to be considered. The regime where the *Kn* number is between 0.001 and 0.1 is known as slip-flow regime [1]. The flow of a gas with a typical mean free path of approximately 100 nm at standard condition inside a microchannel with a dimension of 10 micron would result in a gas

* Corresponding author; e-mail: barbaros@metu.edu.tr, barbaroscetin@gmail.com

flow in a slip-flow regime. Although the equations of continuum mechanics (*i. e*. Navier-Stoke's equations) are valid in this regime the boundary conditions needs to be modified to take into account the non-continuum effects (i.e. rarefaction effects).

The general form of the boundary conditions for velocity and temperature can be written as follows:

$$u - u_{\mathrm{w}} = a_1 \lambda \left(\frac{\partial u}{\partial n} \right)_{\mathrm{wall}} + a_2 \lambda^2 \left(\frac{\partial^2 u}{\partial n^2} \right)_{\mathrm{wall}} + a_3 \lambda^2 \left(\frac{\partial T}{\partial t} \right)_{\mathrm{wall}} \tag{1}$$

$$T - T_{\mathrm{w}} = b_1 \lambda \left(\frac{\partial T}{\partial n} \right)_{\mathrm{wall}} + b_2 \lambda^2 \left(\frac{\partial^2 T}{\partial n^2} \right)_{\mathrm{wall}} \tag{2}$$

where n and t stand for normal and tangential directions, respectively. First terms of the eqs. (1) and (2) are known as first-order boundary conditions, and the second terms are known as second-order boundary conditions. As the modeling moves to the edge of the slip flow regime (*i. e*. Kn approaches 0.1), the inclusion of the second-order terms improves the accuracy of the solution. The last term of the eq. (1) is known as thermal creep, and is also in the order of λ^2 [1]. However for the ease of the solution this term is neglected in this study.

There are two common models for second-order boundary conditions, which were suggested by Deissler [2] and Karniadakis *et al.* [3]. In this study these two models are implemented, and the corresponding coefficients for these two models are tabulated in tab. 1 [1].

Table 1. List of the coefficients used in eqs. (1) and (2)

	a_1	a_2	b_1	b_2
Deissler	1.0	–9/8	$\frac{2-F_T}{F_T}\frac{2\gamma}{\gamma+1}\frac{1}{\mathrm{Pr}}$	$-\frac{9}{128}\frac{177\gamma-145}{\gamma+1}$
Karniadakis and Beskok	1.0	1/2	$\frac{2-F_T}{F_T}\frac{2\gamma}{\gamma+1}\frac{1}{\mathrm{Pr}}$	$\frac{2-F_T}{F_T}\frac{\gamma}{\gamma+1}\frac{1}{\mathrm{Pr}}$

The effect of the viscous dissipation, which is characterized by Brinkman number, and the axial conduction, which is characterized by Peclet number, are also important at microscale [4]. The fluid flow [5, 6] and heat transfer [4, 7-17] inside a micro-conduit was analyzed for different geometries such as circular tube [4, 7, 9, 11, 14-16], parallel plate [10, 12, 14], rectangular channel [17], annular channel [13] using first-order [4, 7, 10-15] and second-order models [16, 17] both analytically [7, 10-14, 16] and numerically [9, 17]. Some studies included the viscous dissipation [4, 9-12, 14, 15, 17] and the axial conduction [10, 14, 15, 17].

In this study, heat transfer for a fluid flow in a microtube with a constant wall heat flux is analyzed including viscous dissipation, axial conduction and rarefaction effects. Second-order slip models are implemented for the rarefaction effects. Closed form solutions are obtained for fully-developed temperature profile and the Nusselt number.

Analysis

The steady-state, hydrodynamically-developed flow with a constant temperature, T_i, flows into the microtube with the constant heat flux at the wall. Introducing the following dimensionless parameters.

$$\eta = \frac{r}{R},\ \xi = \frac{x}{\mathrm{Pe}\cdot R},\ \theta = \frac{T - T_i}{q_w R / k},\ \bar{u} = \frac{u}{u_m},\ \mathrm{Pe} = \mathrm{Re}\cdot\mathrm{Pr},\ \mathrm{Br} = \frac{\mu u_m^2}{q_w R} \tag{3}$$

The governing energy equation including the axial conduction and the viscous dissipation term, and the corresponding boundary condition can be written as:

$$\frac{\bar{u}}{2}\frac{\partial\theta}{\partial\xi} = \frac{1}{\eta}\frac{\partial}{\partial\eta}\left(\eta\frac{\partial\theta}{\partial\eta}\right) + \frac{1}{\mathrm{Pe}^2}\frac{\partial^2\theta}{\partial\xi^2} + 2\mathrm{Br}\left(\frac{\partial\bar{u}}{\partial\eta}\right)^2 \tag{4}$$

$$\begin{aligned} &\theta = 0 && \text{at } \xi = 0 \\ &\theta \to \theta_\infty && \text{as } \xi \to \infty, \\ &\theta \to \text{finite} && \text{at } \eta = 0, \\ &\frac{\partial\theta}{\partial\eta} = 1 && \text{at } \eta = 1, \end{aligned} \tag{5}$$

where $\bar{u}$ is the dimensionless fully-developed velocity profile for the slip-flow regime. By solving the momentum equation together with the slip-velocity boundary condition, u can be determined as:

$$\bar{u} = \frac{u}{u_\mathrm{m}} = \frac{1 - 2\eta^2}{1 + 8a_1\mathrm{Kn} + 16a_2\mathrm{Kn}^2} + 1 \tag{6}$$

The fully-developed temperature profile has the following functional form [18]:

$$\theta_\infty = A\xi + \phi(\eta) \tag{7}$$

where A is constant that needs to determined. Substituting eq. (7) into eq. (4), and integrating once in η-direction results in:

$$\frac{\mathrm{d}\phi}{\mathrm{d}\eta} = \frac{1}{\eta}\int\left(\frac{\bar{u}A}{2} - \frac{32\mathrm{Br}}{\left(1 + 8a_1\mathrm{Kn} + 16a_2\mathrm{Kn}^2\right)^2}\eta^2\right)\mathrm{d}\eta \tag{8}$$

Using the boundary condition at the wall, A can be determined as:

$$A = 32\mathrm{Br}\chi + 4, \quad \chi = \frac{1}{1 + 8a_1\mathrm{Kn} + 16a_2\mathrm{Kn}^2}\cdot \tag{9}$$

Integrating eq. (8) in η-direction, ϕ can be determined as:

$$\phi(\eta) = \frac{A}{8}(\chi + 1)\eta^2 - \left(\frac{A}{16} + 2\mathrm{Br}\chi\right)\chi\eta^4 + B\ln\eta + C \tag{10}$$

where *B* and *C* are arbitrary constants. Using the boundary condition at the microtube center, constant *B* can be determined as zero. In order to get constant *C*, eq. (4) needs to integrated in η-direction from 0 to 1, and in ξ-direction. These integration results in the following equation:

$$\frac{1}{2}\int_0^1 \bar{u}\theta(\eta,\xi)\eta\mathrm{d}\eta = \xi + \frac{1}{\mathrm{Pe}^2}\frac{d}{\mathrm{d}\xi}\left(\int_0^1 \theta(\eta,\xi)\eta\mathrm{d}\eta\right) + \left(\int_0^1 \frac{32Br}{1 + 8a_1\mathrm{Kn} + 16a_2\mathrm{Kn}^2}\eta^3\mathrm{d}\eta\right)\xi \tag{11}$$

constant *C* can be determined by substituting eq. (7) into eq. (11):

$$C = \mathrm{Br}\chi^2\left(\frac{\chi^2}{3} - \chi + \frac{64}{\mathrm{Pe}^2} + \frac{4}{3}\right) + \frac{1}{4}\left(1 - \frac{\chi}{3} + \frac{\chi^2}{6}\right) + \frac{8}{\mathrm{Pe}^2} \tag{12}$$

Fully-developed temperature can be obtained by substituting eq. (10) into eq. (7) as:

$$\theta_\infty(\xi,\eta) = A\xi + \frac{A}{8}(\chi+1)\eta^2 - \left(\frac{A}{16} + 2\mathrm{Br}\chi\right)\chi\eta^4 + C \tag{13}$$

where A and C are given in eqs. (9) and (12). When Kn = Br = *0*, the solution recovers the macrochannel result [19] as:

$$\theta_\infty = 4\xi + \eta^2 - \frac{\eta^4}{4} - \frac{7}{24} + \frac{8}{\mathrm{Pe}^2} \tag{14}$$

Introducing dimensionless quantities, fully-developed Nusselt number can be written as:

$$\mathrm{Nu}_\infty \equiv \frac{h_\infty D}{k} = -\frac{2}{\theta_\mathrm{m} - \theta_\mathrm{w}} \tag{15}$$

where θ_{mean} is the dimensionless mean temperature which is defined as:

$$\theta_\mathrm{m} = 2\int_0^1 \bar{u}\theta_\infty(\eta,\xi)\eta\,\mathrm{d}\eta \tag{16}$$

and θ_{wall} is the wall temperature and can be determined by the implementation of the temperature-jump boundary condition, eq. (2) as:

$$\theta_\mathrm{w} = \theta_\infty(\xi,0) + 2b_1\mathrm{Kn}\left(\frac{\partial\theta}{\partial\eta}\right)_{\eta=1} - 4b_2\mathrm{Kn}^2\left(\frac{\partial^2\theta}{\partial\eta^2}\right)_{\eta=1} \tag{17}$$

Substituting eqs. (13), (17) into eq. (15), Nu_∞ can be determined as:

$$\mathrm{Nu}_\infty = \frac{1}{\dfrac{\mathrm{Br}\chi^2}{6}(2+3\chi+\chi^2) + \dfrac{\chi}{12}\left(1+\dfrac{\chi}{4}\right) + \dfrac{1}{8} + 2b_1\mathrm{Kn} - 4b_2\mathrm{Kn}^2[8\mathrm{Br}\chi(1-5\chi) - 2\chi + 1]} \tag{18}$$

For a macrochannel flow (*i. e.* Kn = Br = *0*, χ = *1*), the solution recovers well-known result of 48/11 [18, pp. 389-390].

Results and discussion

The fully-developed temperature profile and the fully-developed *Nu* is determined by solving the energy equation with the appropriate boundary conditions. Second-order boundary conditions are implemented to include the rarefaction effects. The viscous dissipation and the axial conduction are also included in the analysis. Coefficient b_1 is taken as 1.667 and γ is taken as 1.4 in the calculation of coefficient b_2, which are typical values for air, which is the working fluid in many engineering problems. As seen from eq. (13) fully developed temperature profile is function of Kn, Br, Pe and ξ, however, the fully developed Nu is function of only Kn and Br, and does not depend on Pe which means Pe number only effects the local Nu in the thermal entrance region.

Table 2. Fully-developed Nu for different Kn and Br number values

	Br = 0			Br = 0.1		Br = –0.1	
Kn	1st order model	2nd order model [2]	2nd order model [3]	2nd order model [2]	2nd order model [3]	2nd order model [2]	2nd order model [3]
0.00	4.36	4.36	4.36	3.04	3.04	7.74	7.74
0.02	4.07	4.09	4.07	3.27	3.20	5.47	5.59
0.04	3.75	3.80	3.74	3.38	3.16	4.32	4.59
0.06	3.44	3.50	3.43	3.42	3.02	3.60	3.97
0.08	3.16	3.23	3.16	3.39	2.85	3.08	3.53
0.10	2.90	2.97	2.92	3.31	2.68	2.69	3.20
0.12	2.68	2.73	2.71	3.22	2.52	2.37	2.92

The fully-developed values for different Kn and Br numbers are tabulated in tab. 2. The fully-developed Nu for different Kn and Br numbers is also shown in fig 1. The results for first-order model are also included in the fig. 1. As seen from the figure, the second-order model proposed by Karniadakis *et al.* [3] gives close results to first-order model. However, the second-order model proposed by Deissler [2] gives appreciably deviation from first-order model. For both models deviation from first-order model increases as the rarefaction increases (*i. e.* increasing Kn).

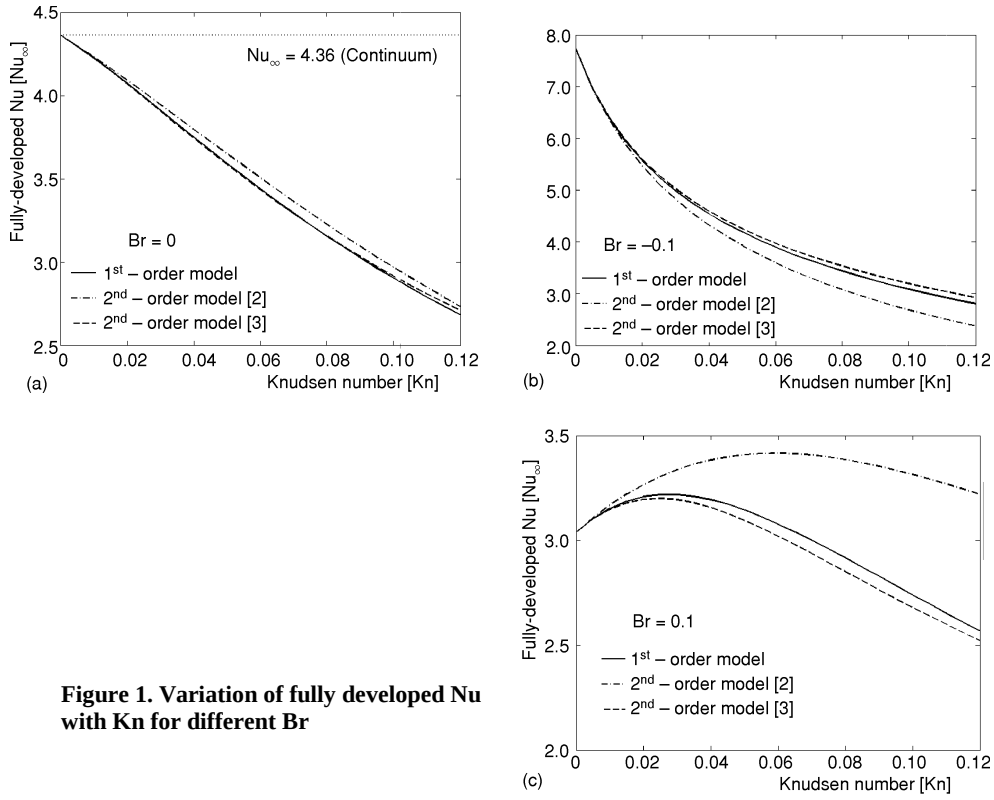

Figure 1. Variation of fully developed Nu with Kn for different Br

Br number has an appreciable effect on Nu value. Positive Br means that the fluid is being heated and negative Br means that the fluid is being cooled. For Br < *0*, second-order model of [2] underestimate the Nu than that of fist-order model, and second-order model of [3] overestimate the Nu than that of fist-order model. For Br > *0*, the situation is *vice-versa*.

In this study only the fully-developed region is considered. Since the length-over-diameter ratio is high for microchannels, in the majority of the channel the flow will be fully-developed. However, in order to see the complete picture, thermally developing region can be analyzed. In that analysis, the superposition method can be utilized and the fully-developed temperature profile can be subtracted from the overall solution and the remaining homogenous equation can be solved by using eigen-function expansion [14]. In the analysis, thermal creep term in the slip-flow boundary condition, eq. (1) is neglected. Inclusion of the thermal creep term in the analysis will be the future research direction.

Nomenclature

Br – Brinkman number (= $\mu u_m^2/q_w R$), [–]
D – tube diameter [m]
F – accommodation factor
h – convective heat transfer coefficient [$Wm^{-2}K^{-1}$]
k – thermal conductivity [$Wm^{-2}K^{-1}$]
Kn – Knudsen number (= λ/L), [–]
L – characteristic length [m]
Nu – Nusselt number (= $h_\infty D/k$), [–]
Pe – Peclet number (= Re·Pr), [–]
Pr – Prandtl number (= ν/α), [–]
q – heat flux [Wm^{-2}]
r – radial coordinate [m]
R – tube radius [m]
Re – Reynolds number (= $u_m D/\nu$), [–]
T – fluid temperature [K]
u – velocity in axial direction [ms^{-1}]
$\overline{u}$ – dimensionless velocity
x – axial coordinate [m]

Greek symbols

α – thermal diffusivity [m^2s^{-1}]
χ – parameter defined in eq. (9)
ϕ – dimensionless temperature
γ – specific heat ratio
η – dimensionless radial coordinate
λ – mean free path [m]
μ – dynamic viscosity [$kgm^{-1}s^{-1}$]
ν – kinematic viscosity [m^2s^{-1}]
θ – dimensionless temperature
ξ – dimensionless axial coordinate

Subscripts

i – inlet
m – mean
T – thermal
w – wall
∞ – fully-developed

References

[1] Karniadakis, G. E., Beskok, A., Micro Flows: Fundamentals and Simulation, Springer-Verlag, New York, 2002
[2] Deissler, R. G., An Analysis of Second-Order Slip Fow and Temperature-Jump Boundary Conditions for Rarefied Gases, *Int. J. Heat Mass Transfer 7* (1964), 6, pp. 681-694
[3] Karniadakis, G. E., Beskok, A., Aluru, N., Microflows and Nanoflows: Fundamentals and Simulation, Springer-Verlag, New York, 2005
[4] Çetin, B., Yazicioglu, A., Kakac, S., Fluid Fow in Microtubes with Axial Conduction Including Rarefaction and Viscous Dissipation, *Int. Comm. Heat Mass Transfer, 35* (2008), 5, pp. 535-544
[5] Colin, S., Lalonde, P., Caen, R., Validation of a Second-Order Slip-Flow Model in Rectangular Microchannels, *Heat Transfer Eng., 25* (2004), 3, pp. 23-30
[6] Aubert, C., Colin, S., High-Order Boundary Conditions for Gaseous Flows in Rectangular Microducts, *MicroscaleThermophys. Eng., 5* (2001), 1, pp. 41-54
[7] Ameel, T. A., *et al*., Laminar Forced Convection in a Circular Tube with Constant Heat Flux and Slip Flow, *MicroscaleThermophys. Eng., 1* (1997), 4, pp. 303-320
[8] Xue, H., Ji, H., Shu, C., Prediction of Flow and Heat Transfer Characteristics in Micro-Couette Flow, *Microscale Thermophysical Eng., 7* (2003), 1, pp. 51-68

[9] Chen, C. S., Kuo, W. J., Heat Transfer Characteristics of Gaseous Flow in Long Mini- and Microtubes, *Numerical Heat Transfer-Part A, 46* (2004), 5, pp. 497-514
[10] Jeong, H. E., Jeong, J. T., Extended Graetz Problem Including Streamwise Conduction and Viscous Dissipation in Microchannels, *Int. J. Heat Mass Transfer, 49* (2006), 13-14, pp. 2151-2157
[11] Aydin, O., Avci, M., Analysis of Micro-Graetz Problem in a Microtube, *Nanoscale and Microscale Thermophysical Engineering, 10* (2006), 4, pp. 345-358
[12] Roy, S., Chakraborty, S., Near-Wall Effects in Micro Scale Couette Flow and Heat Transfer in the Maxwell-Slip Regime, *Microfluid Nanofluid, 3* (2007), 4, pp. 437-449
[13] Duan, Z., Muzychka, Y. S., Slip Flow Heat Transfer in Annular Microchannels with Constant Heat Flux, *J. Heat Transfer, 130* (2008), 092401
[14] Cetin, B., Yazicioglu, A., Kakac, S., Slip-Flow Heat Transfer in Microtubes with Axial Conduction and Viscous Dissipation-An Extended Graetz Problem, *Int. J. Thermal Sciences, 48* (2009), 9, pp. 1673-1678
[15] Cetin, B., Yuncu, H., Kakac, S., Gaseous Flow in Microchannels with Viscous Dissipation, *Int. J. Transport Phenom., 8* (2006), 4, pp. 297-315
[16] Xiao, N., Elsnab, J., Ameel, T., Microtube Gas Flows with Second-Order Slip Flow and Temperature Jump Boundary Conditions, *Int. J. Thermal Sciences, 48* (2009), 2, pp. 243-251
[17] van Rij, J., Ameel, T., Harman, T., An Evaluation of Secondary Effects on Microchannel Frictional and Convective Heat Transfer Characteristics, *Int. J. Heat and Mass Transfer, 52* (2009), 11-12, pp. 2792-2801
[18] Deen, W. M., Analysis of Transport Phenomena, Oxford University Press, Oxford, UK, 1998
[19] Vick, B., Ozisik, M. N., An Exact Analysis of Low Peclet Number Heat Transfer in Laminar Fow with Axial Conduction, *Lett. in Heat Mass Transfer, 8* (1981), 1, pp. 1-10

Paper submitted: July 1, 2010
Paper revised: September 14, 2010
Paper accepted: November 11, 2010